

Zeitschrift: Schweizerische mineralogische und petrographische Mitteilungen =
Bulletin suisse de minéralogie et pétrographie

Band: 77 (1997)

Heft: 1

Artikel: Prograde and retrograde chloritoid zoning in low temperature
metamorphism, Alpi Alpuane, Italy

Autor: Franceschelli, Marcell / Memmi, Isabella / Carcangiu, Gianfranco

DOI: <https://doi.org/10.5169/seals-58468>

Nutzungsbedingungen

Die ETH-Bibliothek ist die Anbieterin der digitalisierten Zeitschriften auf E-Periodica. Sie besitzt keine Urheberrechte an den Zeitschriften und ist nicht verantwortlich für deren Inhalte. Die Rechte liegen in der Regel bei den Herausgebern beziehungsweise den externen Rechteinhabern. Das Veröffentlichen von Bildern in Print- und Online-Publikationen sowie auf Social Media-Kanälen oder Webseiten ist nur mit vorheriger Genehmigung der Rechteinhaber erlaubt. [Mehr erfahren](#)

Conditions d'utilisation

L'ETH Library est le fournisseur des revues numérisées. Elle ne détient aucun droit d'auteur sur les revues et n'est pas responsable de leur contenu. En règle générale, les droits sont détenus par les éditeurs ou les détenteurs de droits externes. La reproduction d'images dans des publications imprimées ou en ligne ainsi que sur des canaux de médias sociaux ou des sites web n'est autorisée qu'avec l'accord préalable des détenteurs des droits. [En savoir plus](#)

Terms of use

The ETH Library is the provider of the digitised journals. It does not own any copyrights to the journals and is not responsible for their content. The rights usually lie with the publishers or the external rights holders. Publishing images in print and online publications, as well as on social media channels or websites, is only permitted with the prior consent of the rights holders. [Find out more](#)

Download PDF: 13.01.2026

ETH-Bibliothek Zürich, E-Periodica, <https://www.e-periodica.ch>

Prograde and retrograde chloritoid zoning in low temperature metamorphism, Alpi Apuane, Italy

by *Marcello Franceschelli¹, Isabella Memmi², Gianfranco Carcangiu³ and Giovanni Gianelli⁴*

Abstract

In the low-temperature metamorphic rocks of the "Breccia di Seravezza" Formation of the Alpi Apuane the chloritoid porphyroblasts are commonly zoned for Mg and Fe. Three kinds of zoning have been detected: (1) type A zoning with Mg/(Mg + Fe) ratio increasing from core to rim; (2) type B zoning with Mg/(Mg + Fe) ratio decreasing from core to rim; (3) type C zoning with Mg/(Mg + Fe) ratio increasing from core to outer core and then decreasing towards the rim. Type A and B zoning have been observed both in pyrophyllite-bearing and pyrophyllite-free samples, while type C zoning occurred only in pyrophyllite-free samples. In some samples chloritoid coexists with chlorite (varying in composition from Mg-Al chamosite to Fe-Al clinochlore) and the K_D Fe/Mg between chloritoid and chlorite range from 5 to 9.27 with an average value of 6.5. The composition of chloritoid and chlorite coexisting with pyrophyllite has been calculated in the range $T \sim 300$ –450 °C and $P = 5$ kbar. From the T - X_{Mg} diagram, type A zoning has been interpreted as evidence of prograde metamorphism, and types B and C as evidence of retrograde metamorphic effect. The chloritoid zoning is discussed in relation to the P-T time path of the low temperature rock of the Alpi Apuane during the Alpine orogeny.

Keywords: chloritoid, Mg–Fe zoning, low-temperature metamorphism, P-T time path, Alpine orogeny, Alpi Apuane, Northern Apennines.

Introduction

Chloritoid is an important rock-forming mineral in Al-rich pelites occurring under a wide range of P-T conditions. Several authors ASHWORTH and EVIRGEN (1984); CHOPIN and SCHREYER (1983); CHOPIN and MONIÉ (1984); CRUICKSHANK and GHENT (1978); GHENT et al. (1987) among others have described Fe–Mg zoning of chloritoid in which the Fe and Mg behave antithetically with little or no change of Mn. No comprehensive model has been proposed to explain the zoning of chloritoid or to relate it to the history of the metamorphic terranes. ASHWORTH and EVIRGEN (1984) interpreted the increasing Mg content from core to rim of chloritoid in pelitic rocks of Lycian Nappe of Turkey as a result of prograde

growth zoning in which the core retained the early formed composition. They also proposed for chloritoid a refractory behaviour in the sense of HOLLISTER (1966).

Low-temperature Triassic rocks from the Autochthon Unit of the Alpi Apuane – informally named "chloritoid schist" – commonly contain chloritoid porphyroblasts with significant Fe–Mg zoning. In this paper, we present the results of a detailed microprobe study on the chemical zoning of the chloritoid and we also examine the chemical relationships between coexisting chloritoid and chlorite. The aim of this study was to investigate the origin and causes of chloritoid zoning and its qualitative use in monitoring the P-T history of low-grade metamorphic rocks of the Alpi Apuane during the Alpine orogeny.

¹ Dipartimento di Scienze della Terra, via Trentino, 51, Università di Cagliari, I-09126 Cagliari, Italy.

² Dipartimento di Scienze della Terra, via delle Cerchia, 3, Università di Siena, I-53100 Siena, Italy.

³ Centro Studi Geominerari e Mineralurgici C.N.R., Piazza d'Armi, I-09126 Cagliari, Italy.

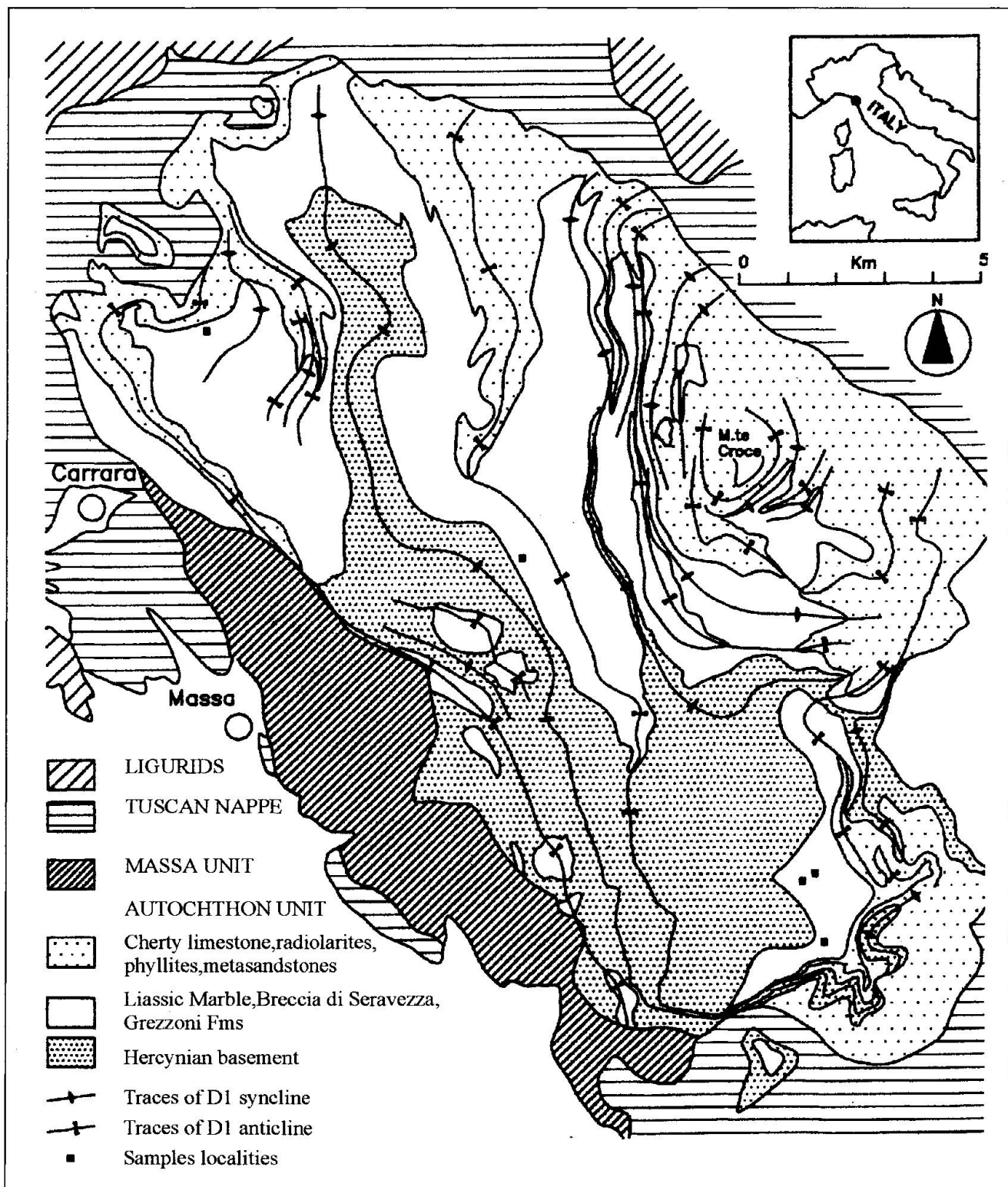
⁴ Istituto Internazionale per le Ricerche Geotermiche, C.N.R., Piazza Solferino, 2, I-56100 Pisa, Italy.

Regional geology

The Alpi Apuane region is a "core complex" type structure (COLI, 1989; CARMIGNANI and KLIGFIELD, 1990) that exposes two main lithotectonic units, the Autochthon and Massa Units beneath

the Tuscan Nappe (Fig. 1). The Autochthon Unit consists of a pre-Alpine basement of volcano-sedimentary nature and a predominantly carbonate cover whose sedimentation age ranges from Permian to Oligocene.

The rocks of the Alpi Apuane record a history



of compression (D_1 folding phase) followed by progressive extensional tectonics (D_2 folding phase). The D_1 phase produced a NW-SE trending fold system associated with an axial plane (S_1) schistosity. The D_2 phase generated E-W and N-NW trending fold systems locally associated with a pervasive axial plane schistosity (S_2) (CARMIGNANI et al., 1978).

Isotopic K/Ar and $^{39}\text{Ar}/^{40}\text{Ar}$ data of about 27 and 12–10 Ma were obtained in sites dominated by the growth of abundant D_1 and D_2 muscovite, respectively (KLIGFIELD et al., 1986).

The widespread occurrence of Al-silicate in the Alpi Apuane rocks allows the delineation of two metamorphic zones with increasing metamorphic grade: the pyrophyllite + quartz zone and the kyanite + quartz zone (Massa Unit). The Autochthon Unit rocks belong to the pyrophyllite + quartz zone (FRANCESCHELLI et al., 1986a), indicating a temperature range between the upper thermal stability limit of kaolinite + quartz (280–300 °C) and the upper thermal stability limit of pyrophyllite + quartz (400–450 °C). The metamorphic pressure at the peak of metamorphism for this zone was estimated at about 4–6 kbar on the basis of geological considerations and the systematic study of the celadonite content of muscovite (FRANCESCHELLI et al., 1986a; COSTAGLIOLA et al., 1992).

Sample description

The "chloritoid schist" samples (Fig. 1) were from the Triassic "Breccia di Seravezza" formation. This formation, located between the "Grezzoni" formation or "Marmi a Megalodonti" formation and the Liassic Marble formation, is characterized by great lithological heterogeneity and lateral variability both in composition and thickness (PANNUTI, 1992). The base of the formation consists of a metabreccia with pelitic or calc-pelitic matrix. The top of the formation comprises a thick (0.5–1 m) layer of "chloritoid schist", which is interpreted as metamorphic equivalent of modern laterites (GIGLIA and TREVISAN, 1967).

The "chloritoid schist" consists of porphyroblasts of chloritoid (40–50% in modal proportion) and sometimes allanite rimmed by epidote s.s. up to 3 mm in length, embedded in a fine-grained matrix of muscovite + quartz \pm chlorite \pm pyrophyllite \pm calcite \pm hematite \pm rutile, zircon, and tourmaline. Some kaolinite relics in the pressure shadows of epidote are sporadically observed. More rarely the chloritoid porphyroblasts are embedded in a matrix of muscovite + pyrophyllite \pm diasporite \pm cookeite \pm margarite + rutile and

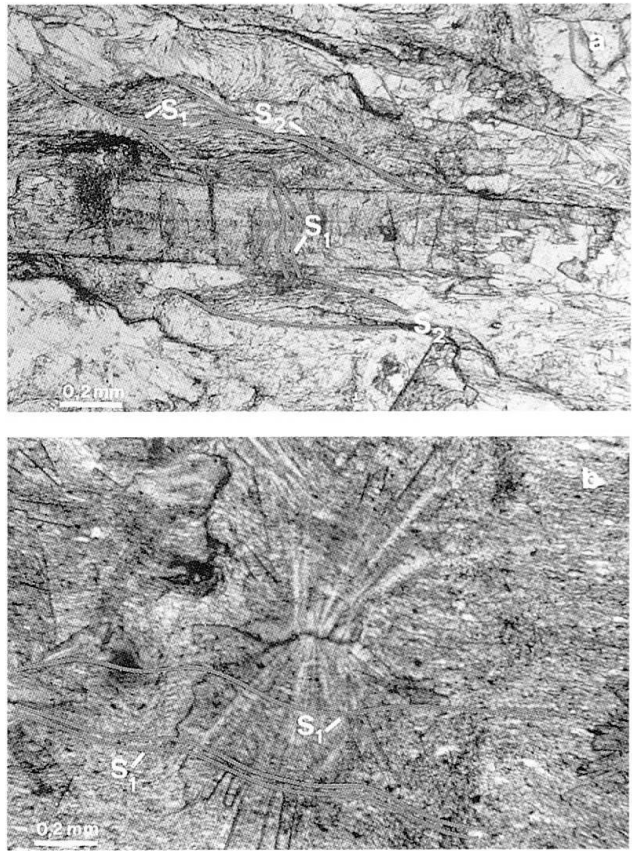


Fig. 2 Photomicrographs showing the relations of chloritoid with S_1 and S_2 schistosity; a) single lath-shaped chloritoid crystal with S-shaped inclusion trails discordant with the external S_1 in the groundmass, b) Rosette in which the S_1 schistosity together with the external S_1 schistosity is gently folded.

hematite. The matrix shows two well-developed schistosity planes S_1 and S_2 . Chlorite (5–10% in modal proportion), muscovite and pyrophyllite occur as small flakes parallel to the S_1 schistosity or as discrete interleaved grains. The S_1 schistosity is generally crenulated and locally transposed by the S_2 schistosity, which is generally defined by the orientation of opaque materials and newly formed phyllosilicates.

Chloritoid generally occurs as single lath-shaped porphyroblasts or as rosettes (Fig. 2 a, b). It usually shows polysynthetic twinning and hour-glass structure. The porphyroblasts preserve (Fig. 2b) gently folded trails of S_1 minerals (quartz, muscovite, pyrophyllite and very rarely chlorite). The porphyroblasts frequently contain opaque mineral inclusions, more abundant in the core region. Microstructural analysis suggests that the chloritoid porphyroblasts began to grow during the final stage of the D_1 deformation and continued to grow until the early stage of D_2 deformation was attained.

Mineral chemistry

Analyses of chloritoid and chlorite were performed with an EDAX-energy dispersive system attached to a Philips 515 Scanning Electron Mi-

croscope using the procedure described by FRANCESCHELLI et al. (1986b). Analyses were also performed with a fully automated ARL-SMQ electron microprobe operating at 20 kV, 20 nA sample current and using a beam spot size of ap-

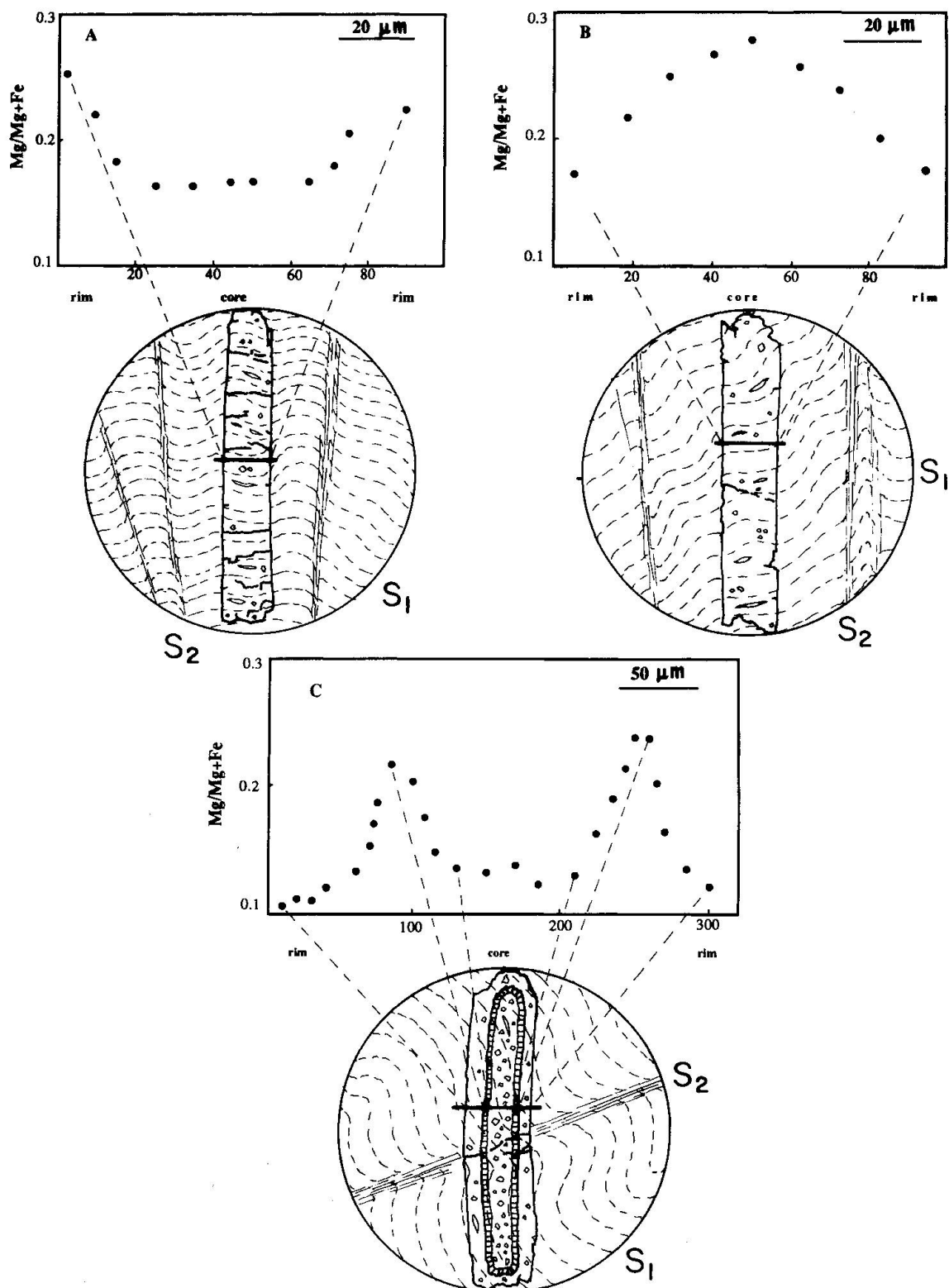


Fig. 3 $Mg/(Mg + Fe)$ profiles across chloritoid; A) representative type A zoning from sample 1; B) representative type B zoning from sample 7; C) representative type C zoning from sample 4.

Tab. 1 Mineral assemblages and representative microprobe analyses for core and rim of chloritoid from seven selected samples from the "Breccia di Seravezza" formation. For sample 4, intermediate rim (r2) composition is also reported. Mineral abbreviations according to KRETZ (1983).

| 1 | | 2 | | 3 | | 4 | | | 5 | | 6 | | 7 | | |
|--------------------------------|-------|-------|-------|-------|-------|------------------|------------------|-------|-------|-------|-------|-------|-------|-------|-------|
| rim | core | rim | core | rim | core | rim ₁ | rim ₂ | core | rim | core | rim | core | rim | core | |
| SiO ₂ | 24.21 | 24.20 | 24.64 | 23.89 | 24.68 | 24.12 | 24.22 | 24.23 | 24.59 | 24.23 | 23.90 | 23.87 | 24.30 | 24.39 | 24.49 |
| Al ₂ O ₃ | 41.07 | 40.92 | 41.11 | 39.96 | 41.10 | 40.87 | 40.40 | 41.47 | 39.47 | 40.71 | 41.16 | 41.05 | 42.54 | 41.05 | 41.45 |
| FeO | 22.94 | 25.83 | 23.16 | 26.95 | 25.08 | 26.09 | 26.69 | 24.23 | 26.58 | 25.38 | 24.46 | 25.32 | 24.09 | 24.59 | 22.75 |
| MgO | 4.24 | 2.69 | 3.32 | 2.01 | 2.73 | 2.07 | 1.90 | 3.75 | 2.28 | 2.17 | 2.67 | 2.40 | 3.45 | 2.81 | 4.79 |
| Total | 92.46 | 93.64 | 92.23 | 92.81 | 93.59 | 93.15 | 93.21 | 93.68 | 92.92 | 92.49 | 92.19 | 92.64 | 94.38 | 92.84 | 93.48 |
| Si | 1.974 | 1.975 | 2.023 | 1.980 | 2.011 | 1.986 | 1.998 | 1.959 | 2.034 | 2.005 | 1.974 | 1.984 | 1.950 | 2.000 | 1.969 |
| Al ^{VI} (M2) | 3.000 | 3.000 | 3.000 | 3.000 | 3.000 | 3.000 | 3.000 | 3.000 | 3.000 | 3.000 | 3.000 | 3.000 | 3.000 | 3.000 | 3.000 |
| Al ^{VI} (M1A) | 0.946 | 0.935 | 0.979 | 0.904 | 0.948 | 0.964 | 0.928 | 0.951 | 0.847 | 0.971 | 1.007 | 0.980 | 1.022 | 0.969 | 0.928 |
| Fe ³⁺ | 0.071 | 0.082 | 0.005 | 0.110 | 0.044 | 0.046 | 0.074 | 0.076 | 0.131 | 0.026 | 0.010 | 0.031 | 0.012 | 0.031 | 0.093 |
| Fe ²⁺ | 1.493 | 1.681 | 1.586 | 1.758 | 1.665 | 1.751 | 1.767 | 1.562 | 1.708 | 1.730 | 1.680 | 1.711 | 1.604 | 1.656 | 1.437 |
| Mg | 0.516 | 0.327 | 0.406 | 0.249 | 0.332 | 0.254 | 0.233 | 0.452 | 0.281 | 0.268 | 0.328 | 0.294 | 0.413 | 0.344 | 0.574 |
| Sum | 2.009 | 2.008 | 1.992 | 2.007 | 1.996 | 2.005 | 2.001 | 2.014 | 1.989 | 1.998 | 2.009 | 2.005 | 2.017 | 2.000 | 2.010 |
| X _{Mg} | 0.257 | 0.163 | 0.204 | 0.124 | 0.166 | 0.127 | 0.117 | 0.224 | 0.141 | 0.134 | 0.163 | 0.147 | 0.205 | 0.172 | 0.285 |
| K _D Fe/Mg cld/chl | | | 5.29 | | 6.79 | | 5.52 | | | 5.78 | | 9.27 | | | |
| Assemblage | Ms | | Ms | | Ms | | Ms | | Ms | | Ms | | Ms | | Ms |
| | Qtz | | Qtz | | Qtz | | Qtz | | Qtz | | Qtz | | Qtz | | Ma |
| | Cld | | Cld | | Chl | | Chl | | Chl | | Chl | | Chl | | Cook |
| | Prl | | Chl | | Cld | | Cld | | Cld | | Cld | | Cld | | Dia |
| | Ep | | Prl | | Ep | | Ep | | Ep | | Ep | | Ep | | Prl |
| | Cc | | Hem | | Cc | | Cc | | Cc | | Cc | | Hem | | Cld |
| | Hem | | Rt | | Hem | | Hem | | Hem | | Rt | | Hem | | Rt |

proximately 3–4 μm . Natural olivine, microcline, anorthoclase, anorthite, augite, ilmenite and chromite were used as standards. The raw data were corrected by ZAF procedure using the Magic IV program (COLBY, 1968).

CHLORITOID

Representative core and rim compositions of chloritoid porphyroblasts from 7 selected samples are reported in table 1. Structural formulae were calculated on the basis of 12 oxygens; Fe³⁺ content was obtained on a stoichiometric basis through the assumption $|4 - M^{3+}| = 2 \cdot |2 - M^{2+}|$ (CHOPIN et al., 1992).

The silicon contents are close to the stoichiometric values of 2 atoms per formula unit (a.p.f.u.). Al_{tot} is generally close to 4.00 a.p.f.u. and ranges from 3.85 to 4.02 a.p.f.u. Fe³⁺ content varies from core to rim in samples 2, 4, 7. With the exception of sample 7, there is a faint negative correlation between Fe³⁺ and Mg variation. Chloritoid is Fe-rich, but with variable Mg content: X_{Mg} = Mg/(Mg + Fe²⁺) ranges from 0.117 to 0.257, irrespective of zoning type; Mn is low (0.1 wt%) and the Cr and Ti contents are negligible.

CHLORITE

Analyses of chlorites in contact with chloritoid are reported in table 2. Structural formulae were calculated on the basis of 28 oxygens; all the Fe was assumed to be Fe²⁺. The cation sums range from 11.4 to 11.95 a.p.f.u. The Mg/(Mg + Fe) ratio ranges from 0.422 to 0.612. The spread of Mg, Fe and Al of chlorite within each sample is lower than ± 0.02 a.p.f.u. Mn, Cr and Ti contents are negligible. According to the AIPEA recommendations the chlorite was classified as Mg-Al chamosite or Fe-Al clinochlore (BAILEY, 1980).

COMPOSITIONAL ZONING IN CHLORITOID

In all the samples chloritoid showed more or less pronounced Fe–Mg zoning. Three types (A, B, C) of chloritoid zoning profiles were found:

Type A zoning: a representative profile (A) is shown in figure 3. This zoning type is characterized by a gradual increase in X_{Mg} from core to rim. X_{Mg} varies from 0.163 to 0.257. This is the most common zoning and it was observed in Prl-free (mineral abbreviations according to KRETZ, 1983; W = water) and Prl-bearing assemblages includ-

Tab. 2 Analyses of chlorite in contact with chloritoid in five samples from the "Breccia di Seravezza" formation (same abbreviations as in Tab. 1).

| | 2 | 3 | 4 | 5 | 6 |
|--------------------------------|--------|--------|--------|--------|--------|
| SiO ₂ | 25.16 | 26.02 | 24.19 | 24.56 | 24.79 |
| Al ₂ O ₃ | 26.87 | 24.84 | 24.80 | 23.67 | 24.78 |
| FeO | 20.23 | 20.85 | 27.48 | 26.07 | 19.39 |
| MgO | 15.77 | 16.06 | 11.22 | 12.08 | 17.33 |
| Total | 88.03 | 87.77 | 87.69 | 87.38 | 86.29 |
| Si | 5.072 | 5.289 | 5.133 | 5.200 | 5.122 |
| Al ^{IV} | 2.928 | 2.711 | 2.867 | 2.800 | 2.878 |
| Al ^{VI} | 3.501 | 3.263 | 3.331 | 3.112 | 3.163 |
| Fe | 3.503 | 3.554 | 4.869 | 4.615 | 3.351 |
| Mg | 4.742 | 4.881 | 3.554 | 4.133 | 5.344 |
| Sum | 11.746 | 11.688 | 11.754 | 11.860 | 11.848 |
| X _{Mg} | 0.575 | 0.578 | 0.422 | 0.475 | 0.615 |

ing the Cld + Chl + Prl AFM low-variance assemblage.

Type B zoning: a representative profile (B) is shown in figures 3 and 4a. This zoning is characterized by decreasing X_{Mg} from core (0.285) to rim (0.172). Type B zoning is less common than type A and it was detected in Prl-free and Prl-Dia-bearing assemblages.

Type C zoning: a representative profile (C) is shown in figure 3 and a backscattered electron image obtained from the same samples in figure 4b. This zoning type is complex: X_{Mg} gradually increases from 0.141 in the core to an outer zone where a maximum value of 0.224 is reached, then abruptly decreases to 0.117 at the rim. The core profile is very similar in shape and X_{Mg} values to a type A zoning profile whereas the outer zone resembles a type B profile. Type C zoning was the least common of the three types and it was observed only in prl-free assemblages.

Discussion

Fe–Mg PARTITIONING BETWEEN CHLORITOID AND CHLORITE

The AFM projection of figure 5 illustrates the compositions of chloritoid rims coexisting with chlorite and/or pyrophyllite in the studied samples. With the exception of sample 6, the tie-lines joining coexisting chloritoid and chlorite are nearly parallel, indicating systematic partitioning of Mg and Fe between the two minerals and suggesting chemical equilibrium.

The partitioning of Fe and Mg between coexisting chloritoid and chlorite can be described by

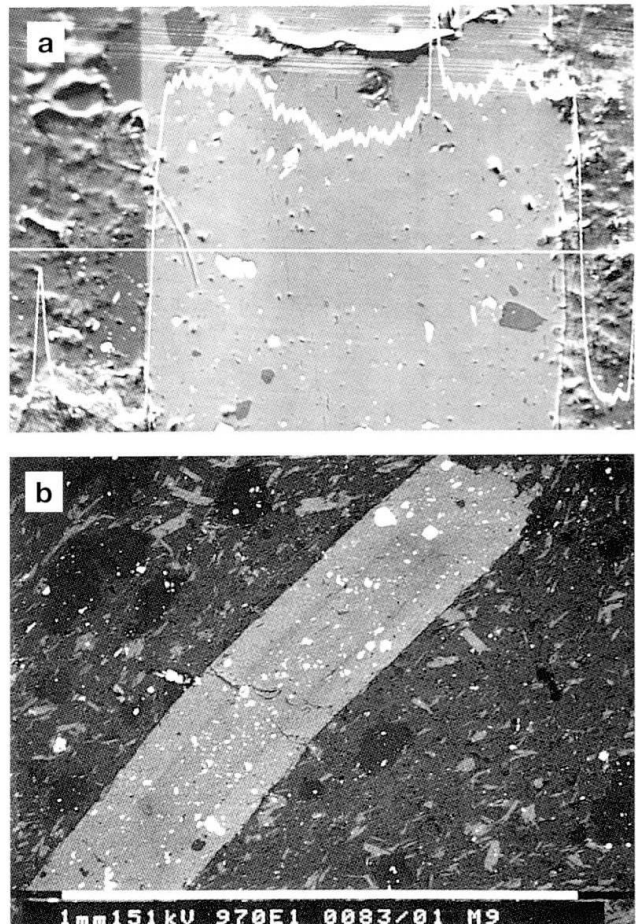


Fig. 4 a) BSE image of chloritoid crystal with type B zoning showing qualitative X-ray Fe-zoning profile; b) BSE image of a zoned lath-shaped chloritoid crystal (sample 4) characterized by type C zoning: note the symmetrical dark bands parallel to the long axis of the crystal corresponding to the maximum value of Mg/(Mg + Fe) ratio.

the distribution coefficient $K_D = (Fe^{2+}/Mg)_{chl}/(Fe_{tot}/Mg)_{chl}$. The $K_D^{chl/chl}$ values in the rocks of the Autochthon Unit range from 5 to 9.27 with an average value of $6.5 \pm 2\sigma = 2.92$.

The samples with the type A chloritoid zoning usually show a smaller range of $K_D^{chl/chl}$ values ($6.1 \pm 2\sigma = 1.6$) with respect to the samples with type B chloritoid zoning. The larger variation in the $K_D^{chl/chl}$ values in the samples with type B chloritoid zoning seems to be due to a relatively Fe-richer composition of chlorite.

The partitioning coefficient Fe–Mg between chloritoid and chlorite has been reported from a number of localities. ASHWORTH and EVIRGEN (1984) give a $K_D^{chl/chl}$ close to 5 (see GHENT et al., 1987) for rocks equilibrated at a temperature of 350 °C. CRUICKSHANK and GHENT (1978) inferred temperature limits of 400 ± 50 °C for $K_D^{chl/chl} = 5.3$ in biotite zone rocks in SE British Columbia.

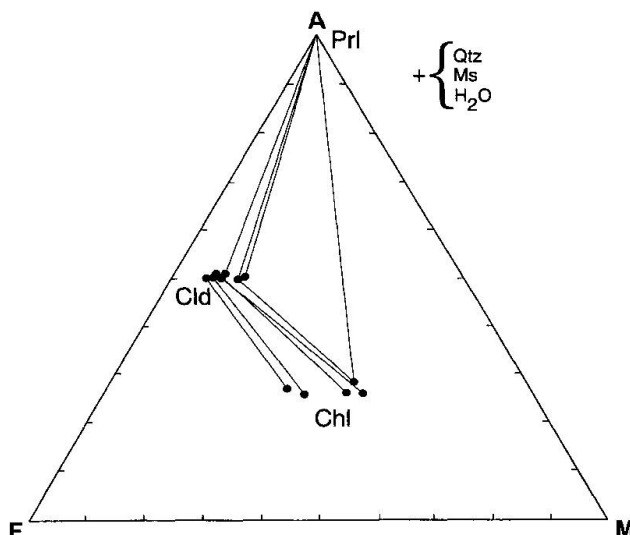


Fig. 5 AFM projection showing the composition of co-existing chloritoid rims and chlorite for rocks (Tab. 1) from the Autochthon Unit of Alpi Apuane.

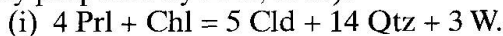
THEYE (1988) reported a $K_D^{\text{cld/chl}} = 6.2 \pm 0.9$ in the high-pressure metasediments from Crete.

The average $K_D^{\text{cld/chl}}$ value of 6.5 for the chloritoid rim and chlorite from the Alpi Apuane were similar to those reported for other supposedly equilibrated chloritoid-chlorite pairs in rocks of similar metamorphic grade.

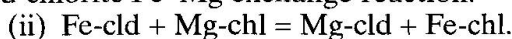
INTERPRETATION OF CHLORITOID ZONING

In the same outcrop and in rocks with similar bulk compositions which have undergone the same metamorphic history, some chloritoid crystals record type A zoning, some others record the type B zoning and a third category records type C, although all chloritoid seems to have nucleated during the prograde part of metamorphic history.

There is little direct evidence of the initial chloritoid-forming reaction. Pyrophyllite and/or chlorite inclusions observed in chloritoid porphyroblasts suggests that chloritoid in $\text{Cld} + \text{Chl} + \text{Prl}$ assemblages were formed by the reaction (originally proposed by ZEN, 1960):



Then we assume that the composition of chloritoid and chlorite is controlled by reaction (i) and/or, in pyrophyllite free-samples, by the chloritoid-chlorite Fe-Mg exchange reaction:



The composition of chloritoid and chlorite co-existing (Fig. 6) with pyrophyllite in a temperature range of 300–450 °C and at pressure of 5 kbar was calculated using the thermodynamic data set of HOLLAND and POWELL (1990). The activities of Fe and Mg-chloritoid have been considered equal to

the mole fractions of iron and magnesium end-members, respectively. For Mg-chlorite (clino-chlorite) and Fe-chlorite (daphnite) we adopted the activity-composition model of WALSHE (1986), assuming ideal mixing to occur over six octahedral and two tetrahedral sites.

The role of oxygen fugacity has been neglected. The pressure effect is negligible below 400 °C, and the temperature uncertainty is quite high ($\pm 50^\circ$) due to the poor quality of the thermodynamic data for Fe-chlorite and Fe-chloritoid (HOLLAND and POWELL, 1990).

Figure 6 allows a semiquantitative estimation of the temperature of equilibration of the chloritoid rim (type A zoning) and chlorite coexisting with pyrophyllite, or in samples with chlorite and chloritoid (type A zoning) but pyrophyllite-free, assuming that pyrophyllite has reacted out. For a chloritoid rim with type A zoning, temperature was probably 300–340 °C (average of 10 samples). This metamorphic temperature appears to be just below that estimated (see Fig. 7) by mineral assemblages. This discrepancy may be mainly attributed to uncertainties in the thermodynamic calculation due to the use of poorly constrained thermodynamic data.

Anyway, whatever the uncertainties in the calculation, figure 6 is useful for determining the

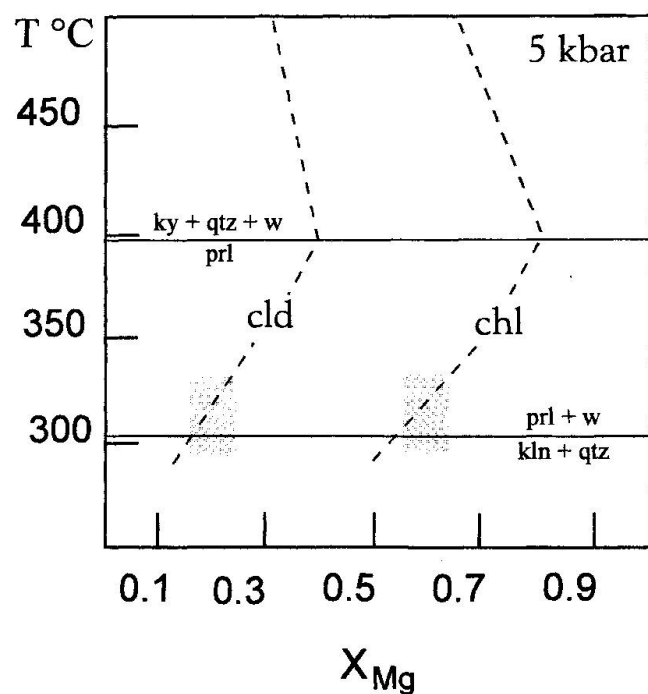


Fig. 6 Isobaric T- X_{Mg} diagram for chloritoid and chlorite calculated for $P = 5$ kbar using the thermodynamic data of HOLLAND and POWELL (1990). The reactions $\text{Kln} + \text{Qtz} = \text{Prl} + \text{W}$ and $\text{Prl} + \text{Qtz} = \text{Ky} + \text{W}$ are also shown. The dashed boxes show the composition of chloritoid rim and chlorite in ten samples.

trend of evolution of X_{Mg} of chlorite and chloritoid with varying temperature.

In light of reaction (i) and taking into account that these rocks belong to the pyrophyllite + quartz zone it should be possible to interpret the variation of X_{Mg} as evidence of temperature increase or decrease during chloritoid growth. If the chloritoid grew when the reaction occurred under prograde conditions, it should result in an increase in X_{Mg} from core to rim and in a decrease of X_{Mg} if the reaction occurred under retrograde conditions. This is not the case in our samples.

As previously noted, chloritoid contains chlorite inclusions, but unfortunately these are too small to yield good analyses. In sample 2, characterized by type A chloritoid zoning, a chlorite included within chloritoid showed $X_{Mg} = 0.47-0.50$; that is, lower than the matrix chlorite ($X_{Mg} = 0.58$). Assuming that the chloritoid and chlorite were always in equilibrium, we can evaluate the ΔT from core-rim chloritoid and chlorite composition. Rimwards this ΔT is about 30 °C. Furthermore the equilibrium temperature for the chloritoid rim (type A profile), should be the temperature of the metamorphic peak (in agreement with COSTAGLIOLA et al., 1992), reached in the early D_2 .

The formation of chloritoid types B and C zoning profiles requires further comments. We could hypothesize some equilibria involving the Fe-phases such as celadonite, epidote or hematite as responsible for these zoning types characterized by variation of the activities of water and oxygen fugacity. Equilibria involving these phases may have different dX_{Mg}/dT slopes, and could determine decreasing X_{Mg} from core to rim of chloritoid. On the other hand, in the studied samples, the content of these phases is very subordinate to the chloritoid and chlorite content. Furthermore, there is no evidence of significant variation of water activity and of oxygen fugacity during chloritoid growth: in fact, hematite and hydrated phases (Prl, Ms, Ep) are included within chloritoid. Then, we can assume that, during the retrograde stage, the chloritoid rim should dissolve. In this case, starting from a chloritoid with a type A zoning or poorly zoned, type B or C zoning may appear in response to net transfer and exchange reactions.

According to SPEAR and PEACOCK (1989) there are two mechanisms and consequently two ways in which a mineral can re-equilibrate: an exchange mechanism and a net transfer mechanism. Each mechanism leaves a different signature on the chemical zoning of minerals in the rocks. In the case of an exchange mechanism the chlorite composition in contact with chloritoid should be characterized by an increase in X_{Mg} , with respect

to the previous composition. In the studied samples, with the exception of samples 5 and 6, where chlorite in contact with chloritoid shows a slight increase of Mg content, in comparison with the matrix chlorite, chlorite composition was found to be essentially homogeneous at the sample scale. This fact may suggest that the formation of the retrograde zoning profile of the chloritoid produced an extensive chemical re-equilibration of chlorite, probably due to the much higher chloritoid content (> 40%) in respect to chlorite content (< 10%).

However, in the presence of the limiting assemblage pyrophyllite-chloritoid-chlorite the composition of chlorite and chloritoid must

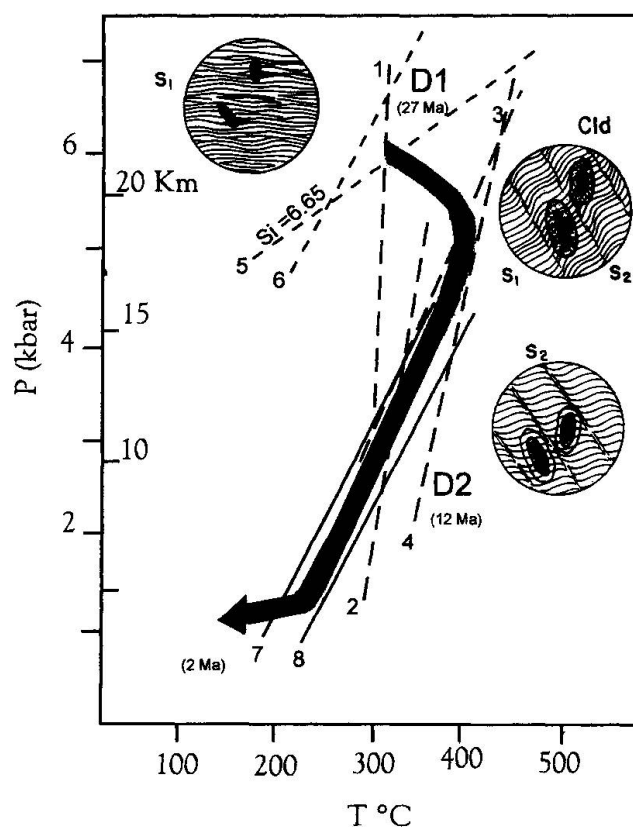


Fig. 7 P-T path of the rocks of the Autochthon Unit (full arrow). Sketches showing the textural development of chloritoid with type C zoning are included. The reconstruction of the P-T path (full arrow) before the peak of metamorphism is based on S_1 mineralogy and zoning data of chloritoid. Reaction 1: $Kln + Qtz = Prl + W$; 2: $Kln = Prl + Dia$; 4: $Prl + Dia = Ky + W$; calculated from thermodynamic data; reaction 3: $Lw + Dia = Mrg + W$ from CHATTERJEE (1976) and reaction 6: $Lw + Gr = Zo + Qtz + W$ from NITSCH (1974). 5. Si (a.p.f.u.) isopleth for the muscovite-phengite series from MASSONNE and SCHREYER (1986). Reactions 7-8: isochores obtained from CO_2 fluid inclusions in barite and fluorite (COSTAGLIOLA et al., 1992). D_1 and D_2 are the first and second folding phases. S_1 and S_2 are the first and second schistosities. Mineral abbreviations according to KRETZ (1983) (see text for explanation).

change continuously, only depending on the temperature, so that we can use chloritoid and chlorite composition to obtain quantitative information about temperature.

In the pyrophyllite-free samples also the bulk composition plays a relevant role in determining the chloritoid and chlorite compositions. As a consequence, the Prl -free samples can only give the trend of evolution of X_{Mg} in chlorite and chloritoid with varying temperature.

P-T time path of the chloritoid rocks

According to COLI (1989); CARMIGNANI and KLIGFIELD (1990); COSTAGLIOLA et al. (1992); ABBATE et al. (1990); BIGAZZI et al. (1988) the rocks in question may have undergone the following metamorphic history: initial burial (at maximum depth of 18–20 km) and compressional deformation (D_1) (27 Ma) was followed by an extension phase D_2 (10–12 Ma). At the end of D_1 and prior to onset of D_2 , with the formation of antiformal stack geometry (middle level crustal attenuation stage of CARMIGNANI and KLIGFIELD, 1990) peak metamorphic conditions were reached.

Mineral assemblages give some additional constraints to the P-T path of chloritoid rocks. In phengite associated with D_1 phase fabric, a maximum celadonite content of $\text{Si} = 6.60\text{--}6.65$ a.p.f.u. has been found by PANNUTI (1992) in the rocks of the "Breccia di Seravezza" formation. Relics of kaolinite observed in some quartz-epidote-bearing samples suggest that the rocks experienced pressure and temperature conditions constrained by the intersection (Fig. 7) of the reactions (1) and (6) and the $\text{Si} = 6.65$ isopleth for the muscovite-phengite series (MASSONNE and SCHREYER, 1987).

The occurrence of the diaspore-margarite-chloritoid-pyrophyllite assemblage gives a maximum temperature of 350–380 °C and pressure of 6 kbar.

After the peak of metamorphism, the temperature decreases as a consequence of retrometamorphic processes related to the uplift and the path is constrained by isochores obtained from CO_2 fluid inclusions in barite and in fluorite that suggest a high dP/dT ratio during exhumation (COSTAGLIOLA et al., 1992). The rocks subsequently underwent a decrease of pressure and temperature and finally isobaric cooling reaching P and T conditions of 1.5 kbar and 120 °C, respectively (ABBATE et al., 1990). Figure 7 shows the P-T path of the Autochthon unit rocks and microstructure development before, during and after the peak of metamorphism.

Microstructural analysis suggests that the chloritoid porphyroblasts began to grow during the final stage of the D_1 deformation and continued to grow until the early stage of D_2 deformation was attained.

From mineral data we know that there was a temperature increase of about 50 °C between D_1 and early D_2 ; that is, during the growth of type A and inner C profiles of chloritoid. The equilibrium temperature for chloritoid rim (type A profile) or outer rim (type C profile) and coexisting chlorite, evaluated to be about 300–340 °C, should be an approximation of the temperature of the metamorphic peak. Subsequently, the metamorphic temperature decrease is recorded in chloritoid crystals by the formation of the type B and C zoning profile.

Worthy of note is that chloritoid crystals in the Alpi Apuane record both a prograde and retrograde portion of the clockwise P-T path, very similar to those typical of collisional orogenic belt.

Conclusions

The chemical zoning of chloritoid makes it a potentially useful mineral in the assessment of the P-T history of the metamorphic rocks of the Alpi Apuane during the Alpine orogeny. The increase of $\text{Mg}/(\text{Mg} + \text{Fe})$ ratio from core to rim seems to record a prograde metamorphism during the D_1 and early D_2 folding phase that affected these rocks. Late P-T retrograde metamorphic evolution of the rocks seems to be recorded in the chloritoid by a rimwards decrease of $\text{Mg}/(\text{Mg} + \text{Fe})$ in several crystals.

In absence of experimental calibration on Fe–Mg chloritoid zoning and chlorite data in the low variance assemblage, the metamorphic temperature can only be semi-quantitatively evaluated.

Acknowledgements

We are grateful to F. Pannuti for invaluable assistance in the field and with microprobe analyses. Precious comments and suggestions by J. Connolly, C. Chopin, T. Theye and O. Vidal were greatly appreciated. Financial support came from Italian Ministry of University and Scientific and Technological Research grants (MURST, to M. F. and I. M.).

References

- ABBATE, E., BALESTRIERI, M., BIGAZZI, G., NORELLI, P. and QUERCIOLI, C. (1990): Apatite fission track datings and the uplift of the Apuan Alps and surrounding regions (Northern Apennines, Italy). Proceed-

- ings of the Seventh International Conference on Geochronology, Cosmochronology and Isotope Geology. Canberra, Australia, 24–29 Sept., 24–29.
- ASHWORTH, J.R. and EVIRGEN, M.M. (1984): Mineral chemistry of regional chloritoid assemblages in the chlorite zone, Lycian nappes, south west Turkey. *Mineral. Mag.*, 48, 159–165.
- BAILEY, S.W. (1980): Summary of recommendations of the AIPEA nomenclature committee. *Can. Mineral.* 18, 143–150.
- BIGAZZI, G., DI PISA, A., GATTIGLIO, M., MECCHERI, M. and NORELLI, P. (1988): La struttura cataclastico-milonitica di Foce di Mosceta, Alpi Apuane Sud-orientali (M. Corchia, Gruppo delle Panie). *Atti Soc. Tosc. Sc. Nat.*, 95, 105–106.
- CARMIGNANI, L., GIGLIA, G. and KLIGFIELD, R. (1978): Structural evolution of the Apuane Alps: An example of continental margin deformation in the Northern Apennines, Italy. *J. Geology*, 86, 487–504.
- CARMIGNANI, L. and KLIGFIELD, R. (1990): Crustal extension in the Northern Apennines: the transition from compression to extension in the Alpi Apuane core complex. *Tectonics*, 9, (6), 1275–1303.
- CHATTERJEE, N.D. (1986): Margarite stability and compatibility relations in the system $\text{CaO}-\text{Al}_2\text{O}_3-\text{SiO}_2-\text{H}_2\text{O}$ as a pressure temperature-indicator. *Am. Mineral.*, 60, 989–993.
- CHOPIN, C. and MONIÉ, P. (1984): A unique magnesiochloritoid-bearing, high pressure assemblage from the Monte Rosa, W Alps: a petrological and $^{40}\text{Ar}/^{39}\text{Ar}$ radiometric studies. *Contrib. Mineral. Petrol.*, 87, 388–398.
- CHOPIN, C. and SCHREYER, W. (1983): Magnesiocarpholite and magnesiochloritoid: two index minerals of pelitic blueschists and their preliminary phase relations in the model system $\text{MgO}-\text{Al}_2\text{O}_3-\text{SiO}_2-\text{H}_2\text{O}$. *Am. J. Sci.*, 283-A, 72–96.
- CHOPIN, C., SEIDEL, E., THEYE, T., FERRARIS, G., IVALDI, G. and CATTI, M. (1992): Magnesiochloritoid, and the Fe–Mg series in the chloritoid group. *Eur. J. Mineral.*, 4, 67–77.
- COLI, M. (1989): Time and mode of uplift of the Apuane Alps metamorphic complex. *Atti Ticinensi Scienze Terra*, 32, 47–56.
- COSTAGLIOLA, P., BENVENUTI, M., LATTANZI, P. and TANELLI, G. (1992): Sollevamento post-metamorfico nella finestra tettonica di S. Anna: Percorso P-T dedotto dai dati delle inclusioni fluide. Abstract, 76° Meeting Società Geologica Italiana. Firenze 21–23 Sept. 1992.
- COLBY, J.W. (1968): MAGIC IV: A computer program for quantitative electron microprobe analysis. Bell Telephone Laboratories, Allenton, P.A. USA.
- CRUICKSHANK, R.D. and GHENT, E.D. (1978): Chloritoid-bearing rocks of the Horsethief Creek Group, southeastern British Columbia. *Contrib. Mineral. Petrol.*, 65, 333–339.
- FRANCESCHELLI, M., LEONI, L., MEMMI, I. and PUXEDDU, M. (1986a): Regional distribution of Al-silicates and metamorphic zonation in the low-grade Verrucano metasediments from the Northern Apennines, Italy. *J. metam. Geol.*, 4, 309–321.
- FRANCESCHELLI, M., MELLINI, M., MEMMI, I. and RICCI, C.A. (1986b): Fine-scale chlorite muscovite association in low grade metapelites from Nurra (SW Sardinia) and the possible mis-identification of metamorphic vermiculite. *Contrib. Mineral. Petrol.*, 93, 137–143.
- GIGLIA, G. and TREVISAN, L. (1967): Genesi e significato paleogeografico delle Brecce tra Grezzoni e Marmi delle Alpi Apuane. *Atti Soc. Tosc. Sc. Nat., Mem.*, 73 (2), 503–517.
- GHENT, E.D., STOUT, M.Z., BLACK, P.M. and BROTHERS, R.N. (1987): Chloritoid-bearing rocks associated with blueschists and eclogites, northern New Caledonia. *J. Metam. Geol.*, 5, 239–254.
- HOLLAND, T.J.B. and POWELL, R. (1990): An enlarged and updated internally consistent thermodynamic dataset within uncertainties and correlations: the system $\text{K}_2\text{O}-\text{Na}_2\text{O}-\text{CaO}-\text{MgO}-\text{MnO}-\text{FeO}-\text{Fe}_2\text{O}_3-\text{Al}_2\text{O}_3-\text{TiO}_2-\text{SiO}_2-\text{C}-\text{H}_2-\text{O}_2$. *J. metam. Geol.*, 8, 89–124.
- HOLLISTER, L.S. (1966): Garnet zoning: an interpretation based on the Rayleigh fractionation model. *Science*, 154, 1647–1651.
- KLIGFIELD, R., HUNZIKER, J., DALLMEYER, R.D. and SCHAMEL, S. (1986): Dating of deformation phases using K–Ar and $^{40}\text{Ar}/^{39}\text{Ar}$ techniques: results from the Northern Apennines. *J. Struct. Geol.*, 8 (7), 781–798.
- KRETZ, R. (1983): Symbols for rock forming minerals. *Am. Mineral.*, 68, 277–279.
- MASSONNE, H.J. and SCHREYER, W. (1987): Phengite geobarometry based on the limiting assemblage with K-feldspar, phlogopite and quartz. *Contrib. Mineral. Petrol.*, 96, 212–224.
- NITSCH, K.H. (1974): Neue Erkenntnisse zur Stabilität von Lawsonit. *Fortschr. Mineral.*, 51, 34–35.
- PANNUTI, F. (1992): Formazione delle Brecce di Seravezza: evoluzione sedimentaria e metamorfica di un orizzonte residuale triassico nelle Alpi Apuane (Toscana). Tesi di Dottorato di Ricerca, Università di Cagliari.
- SPEAR, F. and PEACOCK, S.M. (1989): Metamorphic Pressure-Temperature-Time Paths. Short Course in Geology: vol. 7. Amer. Geophys. Union, Washington, D.C.
- THEYE, T. (1988): Aufsteigende Hochdruckmetamorphose in Sedimenten der Phyllit-Quarziteinheit Kretas und des Peloponnes. Diss. Technische Universität Braunschweig.
- WALSHE, J.L. (1986): A six-component chlorite solution model and the conditions of chlorite formation in hydrothermal and geothermal systems. *Econom. Geol.*, 81, 681–703.
- ZEN, E. AN (1960): Metamorphism of Lower Paleozoic rocks in the vicinity of the Taconic Range in west-central Vermont. *Am. Mineral.*, 45, 129–175.

Manuscript received February 2, 1996; revised manuscript accepted October 16, 1996.